Size effect on shear strength of concrete beams reinforced with FRP bars

F. Matta
Center for Infrastructure Engineering Studies, University of Missouri-Rolla

A. Nanni
Department of Civil, Architectural and Environmental Engineering, University of Miami

N. Galati
Center for Infrastructure Engineering Studies, University of Missouri-Rolla

F. Mosele
Department of Structural and Transportation Engineering, University of Padova

ABSTRACT: The use of glass fiber reinforced polymer (GFRP) bars as internal reinforcement for portions of massive concrete retaining walls to be penetrated by tunnel boring machines (TBMs), commonly referred to as softeyes, is becoming mainstream. The low shear strength and inherent brittleness of GFRP bars greatly facilitate penetration of the TBM, preventing damage to the disc cutters, and eliminating the risk of costly delays. The safe shear design of softeyes and large members in general must account for the strength decrease due to size effect. To date, this phenomenon has not been documented for FRP reinforced concrete (RC). In this paper, the results of laboratory tests on four large-scale concrete beams reinforced with GFRP bars in flexure and shear are presented and discussed. Preliminary results are reported that indicate a decrease in concrete shear strength attributable to size effect, which is offset by an implicit understrength factor in the current ACI 440 design formula. Further experimental research is ongoing to better characterize the extent of size effect in FRP RC.

1 INTRODUCTION

1.1 *Problem statement*

The decrease in concrete contribution to the shear capacity at increasing member depth in steel reinforced beams and slabs has been extensively documented (Kani 1967, Shioya et al. 1989, Collins & Kuchma 1999, Frosch 2000, Lubell et al. 2004). Size effect accrues primarily from the larger width of diagonal cracks as the beam effective depth is increased. Contrasting theories on a sound physical modeling of this phenomenon are being debated, primarily the energetic-statistical scaling (Bažant & Kim 1984, Bažant & Yu 2005a, b) and the crack spacing hypothesis incorporated in the Modified Compression Field Theory (Collins et al. 1996).

The issue is also of fundamental and practical relevance in the design of concrete members reinforced with fiber reinforced polymer (FRP) bars, where deeper and wider cracks due to relatively low elastic modulus of the flexural and, when present, shear reinforcement, as well as reduced dowel action contributed by the tension reinforcement, pose safety concerns that must be addressed. The current ACI "Guide for the Design and Construction of Structural Concrete Reinforced with FRP Bars – ACI 440.1R-06" (ACI 2006) includes a new concrete shear design formula, conceived for application with any reinforcement material. The semi-empirical design equation was rendered in a fringe-type format by calibration on the basis of 370 test results, of which 44 were from FRP reinforced concrete (RC) specimens having a maximum effective depth of 376 mm (Tureyen & Frosch 2003), where size effect is typically negligible. The conservativeness of the design equation for larger FRP RC members remains unproven.

In this paper, the results of the first four large-size glass FRP (GFRP) RC beams tested to date, as part of an extensive research program, are presented and discussed on the basis of the shear strength contribution of the concrete, V_c, and of the transverse reinforcement, V_f. The results indicate the presence of strong size effect on the former. Analysis of the predictions of the ACI formula (ACI 440 2006) compared to experimental results available in the literature and from the present study shows that an implicit understrength factor may offset the strength decrease for effective depths $d \leq 900$ mm, and effective reinforcement ratios ρ_{eff} (i.e. corrected by a factor E_f / E_s to account for the lower FRP stiffness, where E_f = longitudinal elastic modulus of FRP and E_s = elastic modulus of steel) within a range that covers most practical purposes.

1.2 *Practical significance*

A relevant application of large FRP RC members is in softeye openings in temporary retaining walls for tunneling applications. Softeyes are commonly re-

ferred to as the slurry wall sections through which the tunnel boring machine (TBM) penetrates during excavation. The low shear strength and inherent brittleness of glass FRP (GFRP) bars are highly desirable properties for use as softeye reinforcement in lieu of steel. Penetration of the TBMs is greatly facilitated, thereby expediting the field operations, preventing damage to the disc cutters, and eliminating the risk of costly delays. Large-size (Ø32 mm) GFRP bars as shown in Figure 1 are typically required as tensile reinforcement, often in bundles, due to the massive wall dimensions. The technology has been successfully implemented in recent underground projects in North America, Europe, and Asia. Although design principles are fairly well established (Nanni 2003), understanding the implications of size effect is instrumental for the safe design of softeye and other large FRP RC members.

2 DESIGN PROVISIONS

The recently adopted ACI design equation for concrete shear strength is (ACI 440 2006)

$$V_c = \frac{2}{5} k \left(f'_c \right)^{1/2} bd \qquad (1)$$

where $k = [2 \rho_f n + (\rho_f n)^2]^{1/2} - \rho_f n$, ρ_f = FRP flexural reinforcement ratio, n = ratio of E_f to the elastic modulus of concrete, f'_c = cylinder compressive strength of concrete in MPa, b = width of rectangular cross section in mm, and d = effective depth of tension reinforcement in mm. The main parameters affecting V_c are recognized as the axial stiffness of the flexural reinforcement, and the concrete tensile strength, herein assumed proportional to $(f'_c)^{1/2}$ (ACI 318 2005).

Size effect is not explicitly accounted for in Equation 1. Conversely, specific size effect parameters are incorporated in the following design algorithms. For $d \geq 300$ mm, the Canadian Standard Association (CSA 2004) and ISIS Canada (ISIS 2001) recommend

$$V_c = \left(\frac{130}{1000+d} \right) \lambda \phi_c \left(f'_c \right)^{1/2} bd$$
$$\geq 0.008 \, \lambda \phi_c \left(f'_c \right)^{1/2} bd \qquad (2)$$

and

$$V_c = \left(\frac{E_f}{E_s} \right)^{1/2} \left(\frac{260}{1000+d} \right) \lambda \phi_c \left(f'_c \right)^{1/2} bd$$
$$\geq 0.1 \left(\frac{E_f}{E_s} \right)^{1/2} \lambda \phi_c \left(f'_c \right)^{1/2} bd \qquad (3)$$

respectively. The provisions were adopted from the

Canadian standard for steel RC (CSA 1994), where λ = modification factor for concrete density = 1 for normal density concrete, and ϕ_c = resistance factor for concrete = 0.83 when no safety factor is applied to predict experimental results for comparison purposes with ACI, to account for different material safety factors for concrete.

The Institution of Structural Engineers (ISE 1999) recommends

$$V_c = 0.79 \left(100\rho_{eff} \right)^{1/3} \left(\frac{400}{d} \right)^{1/4} \left(\frac{f_{cu}}{25} \right)^{1/3} bd \qquad (4)$$

regardless of beam depth, where f_{cu} = cube compressive strength of concrete. Similarly, the Japanese Society of Civil Engineers (JSCE 1997) proposes

$$V_c = 0.2 \left(100\rho_{eff} \right)^{1/3} \left(\frac{1000}{d} \right)^{1/4} \left(f'_{cd} \right)^{1/3} bd \qquad (5)$$

where f'_{cd} = cylinder compressive strength of concrete, with $(100\rho_{eff})^{1/3} \leq 1.5$, $(1000 \text{ mm} / d)^{1/4} \leq 1.5$ being the size effect parameter based on Weibull statistical theory, and $(f'_c \text{ MPa}^2)^{1/3} \leq 3.6$ MPa.

3 EXPERIMENTAL STUDY

3.1 Specimen design

Four large-size beams were designed according to the ACI 440 guide (ACI 440 2006) and constructed. The cross section and reinforcement layout of Specimens I-1, I-2, II-1 and II-2, are illustrated in Figure 2. The overall height of 978 mm and effective depths were selected as replicate of typical full-scale softeyes, thereby providing dimensions where size effect typically becomes of concern in case of steel RC.

Figure 1. Ø32 mm GFRP reinforcing bar.

Flexural reinforcement consisting of Ø32 mm bars was designed to obtain a nominal GFRP reinforcement ratio ρ_f = 0.59% for Specimens I-1, I-2 and II-1. The value corresponds to ρ_{eff} = 0.12%, thus below the minimum ρ_{eff} = 0.15% in studies reported in the literature and used to calibrate the ACI design equation (Tureyen & Frosch 2003), and yet representative of lower-bound real-case scenarios. Bundles of three Ø32 mm bars were used for Specimen II-2, as often encountered in practice, with ρ_f = 0.89% and ρ_{eff} = 0.17%.

Since at least minimum shear reinforcement is required in most concrete structures, Specimen I-1 was designed to study size effect under such condition, as well as the effectiveness of shear reinforcement in providing postcracking strength. U-shaped Ø16 mm GFRP bars were arranged in the form of closed stirrups spaced at $s \approx s_{min}$ = 406 mm on-center, where $s_{min} = A_{fv}$ min(f_{fv}, f_{fb}) / $(0.35b)$ × mm^2 / N, with A_{fv} = area of transverse reinforcement within s_{min}, f_{fv} = 0.004E_f to account for loss of aggregate interlock, and f_{fb} = strength of bent portion of FRP stirrups. The nominal shear strength, V_n, and the shear force associated with the nominal flexural strength, $V(M = M_n)$, were 253.8 kN and 373.1 kN, respectively, assuming f'_c = 27.6 MPa, and bar strength and axial modulus of 510.2 MPa and 40.7 GPa for the longitudinal reinforcement, and 655 MPa and 40.7 GPa for the shear reinforcement. Shear failure was expected.

Spacing of the shear reinforcement was reduced to 152 mm for Specimens I-2, II-1 and II-2 to further assess the effectiveness of shear reinforcement in providing the required postcracking strength, as well as mitigating the size effect on V_c (Bažant & Sun 1987). Specimen II-1 is replicate of two I-2 sections cast side-by-side and provides a valid counterpart to Specimen I-2, since beam width has negligible effect on V_c (Kani 1967, Sherwood et al. 2006). For Specimens I-2, II-1 and II-2, V_n = 487.0 kN, 974.0 kN and 1390.0 kN, respectively, thus exceeding $V(M = M_n)$ = 373.1 kN, 746.2 kN and 1105.3 kN. The expected failure was flexural due to rupture of the longitudinal reinforcement for Specimens I-2 and II-1, and concrete crushing for Specimen II-2.

The total length of each beam was 9.15 m. An anchorage length of 915 mm was provided past the end supports to prevent bar slip.

3.2 Materials

E-glass/vinyl ester GFRP bars were used to construct the reinforcement cages for the specimens. Average tensile strength and elastic modulus of eight Ø32 mm bar samples were f_{fu} = 462.2 MPa and E_f = 40.7 GPa for Specimens I-1 and I-2, and f_{fu} = 510.2 MPa and E_f = 38.0 GPa for Specimens II-1 and II-2. Average tensile strength and elastic modulus of six Ø16 mm stirrup samples were f_{fu} =

690.0 MPa and E_f = 40.2 GPa, respectively.

Normal weight concrete was used, with average compressive strength f'_c = 38.8 MPa, 35.4 MPa, 29.0 MPa and 31.5 MPa for Specimens I-1, I-2, II-1 and II-2, respectively, as per cylinder tests performed in accordance with ASTM C 39 at the time of testing.

3.3 Test setup

The beams were tested in four-point bending, with shear span a = 2743 mm, thus providing a ratio a / d = 3.1 to obtain a lower-bound value for V_c, and constant moment region of 1829 mm. Assemblies including steel cylinders between flat or grooved plates were arranged at the supports in such a manner to simulate a simple support and a hinged support, respectively, and at the loading sections to simulate hinges. Plywood sheets of 6 mm thickness were interposed between the steel plates and the concrete surface at the supports and loading sections. The loads were applied via manually operated hydraulic actuators with capacity of 1780 kN, and measured with an 890 kN load cell placed under each concentrated load.
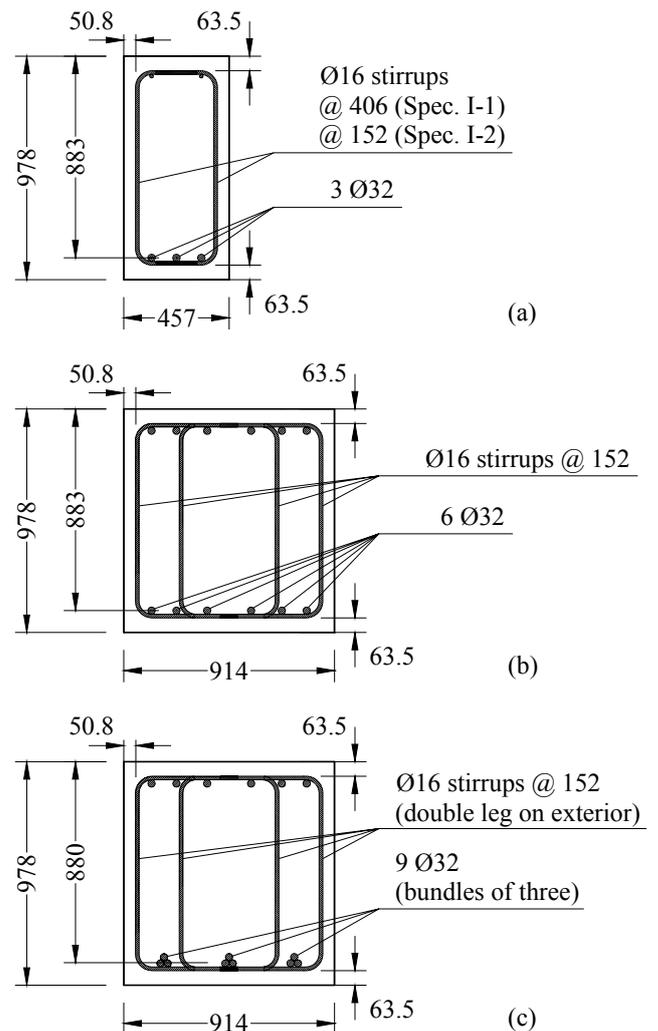

Figure 2. Cross section of GFRP RC Specimens I-1 and I-2 (a), II-1 (b), and II-2 (c). Dimensions in mm.

Direct current voltage transformer (DCVT) sensors and string transducers were used to measure displacements along the length of the beam, at the supports, and at the ends of the flexural reinforcement to capture bar slip. Several strain gauges were used to measure strain in the flexural reinforcement along the beams, in the concrete in compression at midspan, and in the stirrups along the shear spans.

4 RESULTS AND DISCUSSION

4.1 Concrete shear strength

It was found that the difference between the load at which the first inclined ($\geq 45°$) shear crack formed, V_{cr}, and the ultimate strength in six FRP and three steel RC beams without shear reinforcement lay within the 2% - 10% range, except in one instance where the difference was 17% for a GFRP RC specimen with ρ_{eff} = 0.19% and d = 360 mm (Tureyen & Frosch 2002). In the analysis of the test results reported herein, the observed V_{cr} was taken as an acceptable indication of a lower bound for V_c (Frosch 2000). In general, relatively larger gaps in the load-deflection curve accompanied by strain increase in the stirrups were observed at the correspondent load levels.

Table 1 compares V_{cr} for each specimen, including the contribution of self-weight computed at a distance d from the center line of the supports, with the predicted V_c per the guidelines reported in Section 2. The average ratio V_{cr} / V_c is 1.11, 0.90, 1.17, 0.88 and 1.02 for ACI 440 (2006), CSA (2004), ISIS (2001), ISE (1999) and JSCE (1997), respectively. It is seen that the predictions per ACI 440 (2006) cannot be seen as unconservative, despite the absence of any size effect parameter in the formulation. The seeming contradiction is explained by the presence of an implicit understrength factor introduced in Equation 1 (ACI 440 2006). The formula was calibrated by setting K as a constant (2 / 5) to define a simple and conservative design tool applicable irrespectively of the reinforcement material, being such factor theoretically expressed from equilibrium considerations as

$$K = \left(16 + \frac{4\sigma_m}{3\sqrt{f_c'}}\right)^{1/2} \quad (6)$$

where σ_m = concrete stress in extreme compression fiber of uncracked section (Tureyen & Frosch 2003). For values $\rho_{eff} \leq 0.8\%$, i.e. within a typical design range for under- and over-reinforced FRP RC members, the increase in K resulting from higher flexural stresses σ_m in cracked, lightly reinforced sections, determines significantly higher safety factors with respect to steel RC sections. Such result was desirable due to the relatively small number of test results

available to validate the proposed design equation. This is clearly shown in Figure 3, where the ratio between the experimental and the theoretical V_c for Specimens I-1, I-2, II-1 and II-2 and other 52 FRP RC beams found in the literature (Zhao & Maruyama 1995, Deitz et al. 1999, Alkhrdaji et al. 2001, Yost et al. 2001, Tureyen & Frosch 2002, Razaqpur et al. 2004, El-Sayed et al. 2005, 2006) is plotted against ρ_{eff} and d. Since V_{cr} is considered for the results from the present investigation, the corresponding points are plotted including a +17% bar to indicate a reasonable upper bound for V_c.

Formation of the first inclined crack occurred at loads V_{cr} of 1.02, 1.19, 0.98 and 1.25 times the predicted V_c according to ACI 440 (2006) in Specimens I-1, I-2, II-1 and II-2, respectively. Even considering the +17% upper bound for V_c, such values are at least 24% smaller than one would expect at similar levels of ρ_{eff} when size effect is neglected, as illustrated in Figure 3a. This is further substantiated in Figure 3b, as clearly higher experimental versus predicted V_c ratios than that of the present study were reported in the literature for FRP RC specimens having $d \leq 376$ mm, irrespectively of the reinforcement ratio.
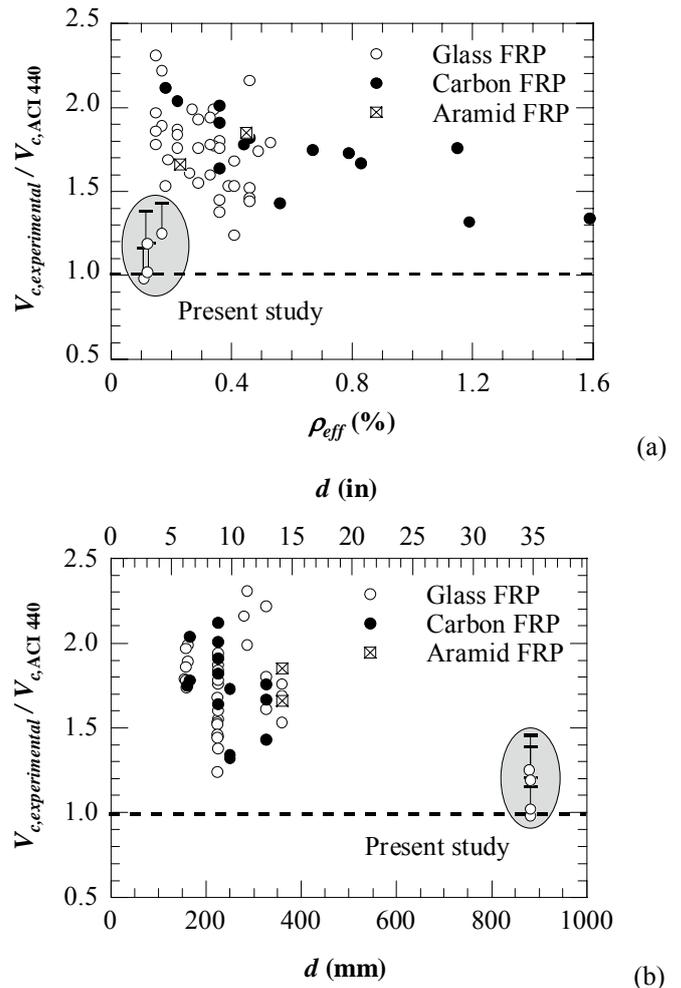

(a)

(b)

Figure 3. Comparison of experimental and theoretical (ACI 440 2006) V_c in FRP RC members in literature based on effective reinforcement ratio (a) and rectangular section depth (b).

Table 1. Shear force at formation of primary shear crack and V_c per existing guidelines.

| Specimen | I-1 | I-2 | II-1 | II-2 |
	kN	kN	kN	kN
Test	127.0	144.7	220.0	344.4
ACI (2006) – Eq. 1	124.8	121.8	223.7	275.7
CSA (2004) – Eq. 2	166.9	159.3	288.4	299.8
ISIS (2001) – Eq. 3	130.0	124.1	217.0	225.9
ISE (1999) – Eq. 4*	160.8	155.9	285.1	335.2
JSCE (1997) – Eq. 5	139.0	134.7	246.4	289.7

* Ratio of cylinder to cube compressive strength of 0.75 assumed.

The presence of an implicit understrength factor in Equation 1 (ACI 440 2006) for relatively small values of ρ_{eff}, commonly encountered in FRP RC, can be also observed in Figure 4 in the case of large-size cross sections. The range of experimental to predicted V_c for the GFRP RC specimens in the present study tends to lie above that for other 24 large-size steel RC beams in the literature (Kani 1967, Taylor 1972, Kawano & Watanabe 1997, Yoshida 2000, Cao 2001, Angelakos et al. 2001, Lubell et al. 2004), which had d, a / d and ρ in the range 0.9 - 2.0 m, 2.8 - 3.0 and 0.50 - 2.72%, respectively, and were tested in either three- or four-point bending.

According to the test results from Specimens I-1, I-2, II-1 and II-2, it also appears that the effect of transverse reinforcement on V_c is negligible for any practical purposes, in agreement with a classical assumption in steel and FRP RC design.

4.2 Contribution of shear reinforcement

Additional shear strength to that of the concrete is provided by the transverse reinforcement upon its engagement once crossed by a diagonal crack. ACI 440 (2006) follows a common straightforward design approach where such contribution is expressed in the form
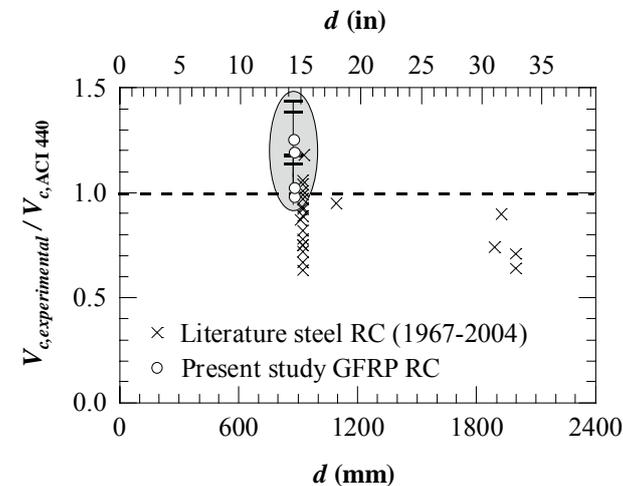
Figure 4. Comparison of experimental and theoretical (ACI 440 2006) V_c in large-size steel RC specimens in literature and GFRP RC specimens in present study.

$$V_f = A_{fv} \min\left(f_{fv}, f_{fb}\right)\frac{d}{s} \qquad (7)$$

thereby assuming formation of the failure crack at a 45° angle. Since the ratio d / s is not truncated and rendered as an integer number, partial contribution of the stirrups is also admissible, although difficult to justify from a physical standpoint.

Figure 5 shows the load-displacement response of Specimens I-1, I-2 and II-1. Load is measured at the loading section in the beam half where failure occurred. Displacement is measured at the correspondent section of maximum deflection.
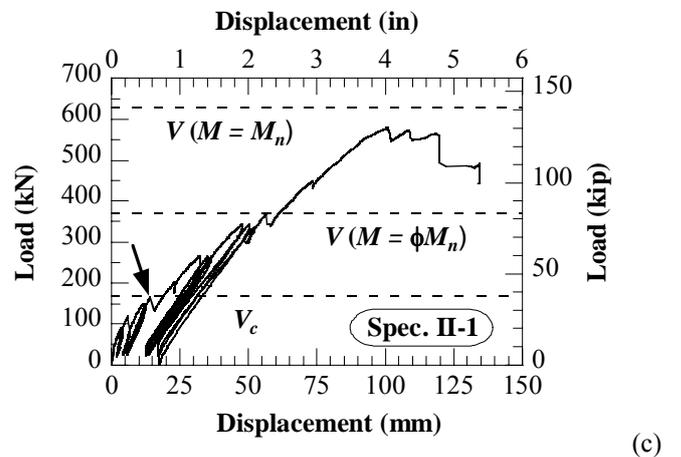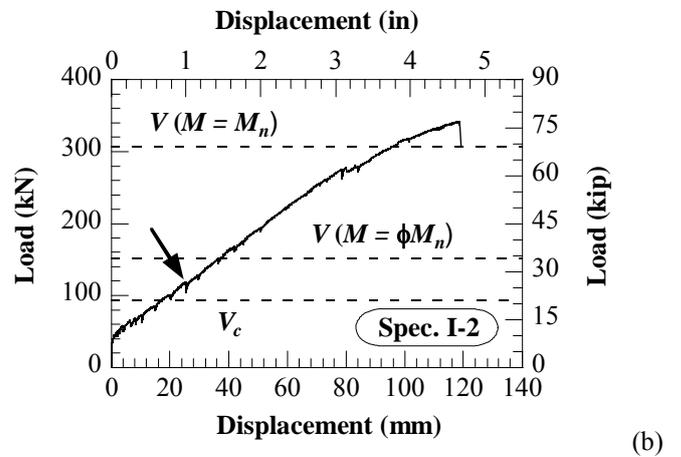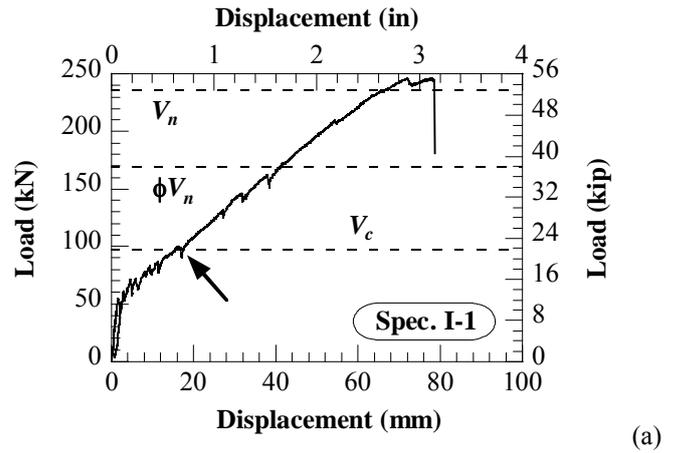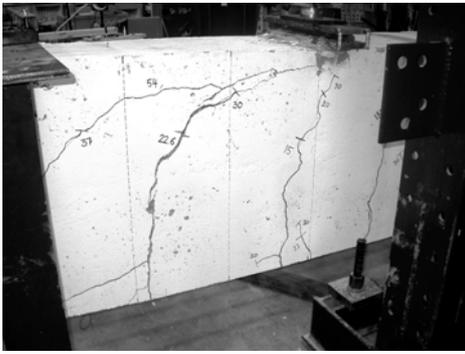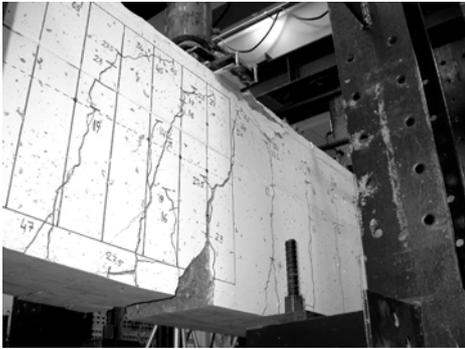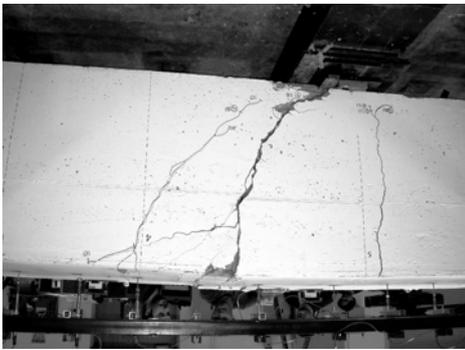
Figure 5. Load-displacement response of Specimens I-1 (a), I-2 (b), and II-1 (c). Arrows indicate formation of primary shear crack.
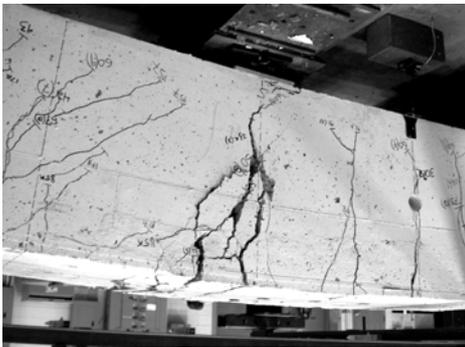
(a)

(b)

(c)

(d)

Figure 6. Photos of failure crack in Specimens I-1 (a), I-2 (b), II-1 (c) and II-2 (d).

Propagation of the primary shear crack deep into the compression zone resulted in failure of Specimen I-1 at a load of 245.5 kN (Figure 6a). The contribution of the GFRP stirrups allowed to attain a total shear strength including self-weight at a distance d from the supports of 273.8 kN > V_n = 263.1 kN. The significant size effect on V_c is offset by the implicit understrength factor identified in the design equation, before application of the design strength reduction factor $\phi = 0.75$ to V_n (ACI 440 2006).

Specimens I-2, II-1 and II-2 were designed to fail in flexure, relying upon the additional strength provided by the closely spaced stirrups. In the case of Specimen I-2, the moment capacity was attained at a load of 341.2 kN, above $V(M = M_n)$ = 305.0 kN and well in excess of the design strength at $M = \phi M_n$, where $\phi = 0.55$ for under-reinforced FRP RC sections (ACI 440 2006). Bar rupture occurred at 305 mm outwards from the nearby loading section (Figures 6b and 7a) due to the combination of tensile and shear stress. However, Specimen II-1 failed in shear compression at a load of 576.5 kN (Figure 5c), fairly close to its nominal strength in flexure. In fact, inspection of the flexural reinforcement upon removal of the surrounding concrete showed some delamination on the surface of the GFRP bars (e.g. in Figure 7b) a clear sign of impending bar rupture. Ultimately, the stirrups contribution in Specimens I-2 and II-1 allowed to exceed the design strength. Nevertheless, the differences in failure mode between the two parent beams calls for further investigation on the effectiveness of shear reinforcement in providing the assumed design strength contribution V_f.

(a)

(b)

(c)

Figure 7. Photos of longitudinal Ø32 mm GFRP bars at failure section in Specimens I-2 (a), II-1 (b) and II-2 (c).

Specimen II-2 reached its moment capacity at a load of 861.7 kN, again fairly close to $V(M = M_n) = 960.3$ kN and well above $V(M = \phi M_n) = 505.8$ kN. Failure mode was rupture of the longitudinal bars (Figures 6d and 7c), which is not surprising given the GFRP reinforcement ratio of 0.95 times the value of balanced failure as computed using the material properties determined experimentally (1.05 in original design), and the concrete strain in the equivalent compression stress block at failure typically greater than the 3000 µε assumed in design. Further research is needed to characterize the influence, if any, of bundled reinforcement on the structural response of FRP RC members.

5 CONCLUDING REMARKS

Preliminary results have been presented from a pilot investigation aimed at assessing the current ACI 440 (2006) shear design provisions in the case of large-size GFRP RC members, which are increasingly being used worldwide in geotechnical applications, such as softeyes for tunnel excavation, and retaining walls. The following conclusions can be drawn:

1 The concrete shear strength appears to be strongly affected by size effect. With respect to scaled counterparts in the literature, strength reduction of at least 24% has been observed in beams with effective depth of about 880 mm and FRP reinforcement ratio of 0.59% and 0.89%, commonly encountered in practice due to the relatively small axial modulus of GFRP bars.

2 Negligible difference on concrete shear strength has been noted in sections with increased amount of shear reinforcement, in agreement with a classical assumption in steel and FRP RC design.

3 The definition of a simple and conservative design equation for concrete shear strength introduced an implicit understrength factor that offsets size effect. At present, adoption of less conservative approaches should not be considered without explicitly addressing size effect.

The conclusions on size effect based on this study must be further substantiated with results from experiments on large-size FRP RC beams without shear reinforcement, which are ongoing as part of a more extensive research program.

Further research is also needed to evaluate the conservativeness of the design provisions for the stirrups contribution to the shear strength, and for the use of bundled longitudinal FRP reinforcement.

REFERENCES

Alkhrdaji, T., Wideman, M., Belarbi, A. & Nanni, A. 2001. Shear strength of GFRP RC beams and slabs. In J. Figueiras, L. Juvandes & R. Furia (eds.), *Composites in Construction – CCC 2001; Proc. intern. conf., Porto, Portugal, 10-12 October 2001*: 409-414.

American Concrete Institute (ACI) Committee 318 2005. *Building code requirements for structural concrete – ACI 318-05*. Farmington Hills, MI: ACI.

American Concrete Institute (ACI) Committee 440 2006. *Guide for the design and construction of structural concrete reinforced with FRP bars – ACI 440.1R-06*. Farmington Hills, MI: ACI.

Angelakos, D., Bentz, E.C. & Collins, M.P. 2001. Effect of concrete strength and minimum stirrups on shear strength of large members. *ACI Structural Journal* 98(3): 290-300.

Bažant, Z.P. & Kim, J.-K. 1984. Size effect in shear failure of longitudinally reinforced beams. *ACI Journal* 81(5): 456-468.

Bažant, Z.P. & Sun, H.-H. 1987. Size effect in diagonal shear failure: influence of aggregate size and stirrups. *ACI Materials Journal* 84(4): 259-272.

Bažant, Z.P. & Yu, Q. 2005a. Designing against size effect on strength of reinforced concrete beams without stirrups: I. Formulation. *Journal of Structural Engineering* 131(12): 1877-1885.

Bažant, Z.P. & Yu, Q. 2005b. Designing against size effect on strength of reinforced concrete beams without stirrups: II. Verification and calibration. *Journal of Structural Engineering* 131(12): 1886-1897.

Canadian Standard Association (CSA) 1994. *Design of concrete structures – CAN/CSA-A23.3-94*. Mississauga, Canada: CSA.

Canadian Standard Association (CSA) 2004. *Design and construction of building components with fibre reinforced polymers – CAN/CSA-S806-02*. Mississauga, Canada: CSA.

Cao, S. 2001. Size effect and the influence of longitudinal reinforcement on the shear response of large reinforced concrete members. *MASc Thesis*. Toronto, Canada: Department of Civil Engineering, University of Toronto.

Collins, M.P. & Kuchma, D. 1999. How safe are our large, lightly reinforced concrete beams, slabs, and footings?. *ACI Structural Journal* 96(4): 482-490.

Collins, M.P., Mitchell, D., Adebar, P. & Vecchio, F.J. 1996. A general shear design method. *ACI Structural Journal* 93(1): 36-45.

Deitz, D.H., Harik, I.E. & Gesund, H. 1999. One-way slabs reinforced with glass fiber reinforced polymer reinforcing bars. In C.W. Dolan et al. (eds.), *Fiber Reinforced Polymer Reinforcement for Reinforced Concrete Structures – FRPRCS-4, ACI SP-188; Proc. int. conf., Baltimore, MD, 31 October–5 November 1999*: 279-286. Farmington Hills, MI: ACI.

El-Sayed, A.K., El-Salakawy, E.F. & Benmokrane, B. 2005. Shear strength of one-way concrete slabs reinforced with FRP composite bars. *Journal of Composites for Construction* 9(2): 147-157.

El-Sayed, A.K., El-Salakawy, E.F. & Benmokrane, B. 2006. Shear strength of FRP-reinforced concrete beams without transverse reinforcement. *ACI Structural Journal* 103(2):

235-243.

Frosch, R.J. 2000. Behavior of large-scale reinforced concrete beams with minimum shear reinforcement. *ACI Structural Journal* 97(6): 814-820.

Institution of Structural Engineers (ISE) 1999. *Interim guidance on the design of reinforced concrete structures using fibre composite reinforcement*. London, UK: ISE.

Intelligent Sensing for Innovative Structures (ISIS) Canada Research Network 2001. *Reinforcing Concrete Structures with Fibre Reinforced Polymers (FRPs) – ISIS Design manual No. 3*. Winnipeg, Canada: ISIS.

Japan Society of Civil Engineers (JSCE) 1997. *Recommendation for Design and Construction of Concrete Structures using Continuous Fiber Reinforcing Materials*. Tokyo, Japan: JSCE.

Kani, G.N.J. 1967. How safe are our large reinforced concrete beams?. *ACI Journal* 64(3): 128-141.

Kawano, H. & Watanabe, H. 1997. Shear strength of reinforced concrete columns – Effect of specimen size and load reversal. In *Proc. 2nd Italy-Japan Workshop on Seismic Design and Retrofit of Bridges, Rome, Italy, 27-28 February 1997*: 141-154.

Lubell, A., Sherwood, T., Bentz, E. & Collins, M. 2004. Safe shear design of large, wide beams. *Concrete International* 26(1): 66-78.

Nanni, A. 2003. North American design guidelines for concrete reinforcement and strengthening using FRP: principles, applications and unresolved issues. *Construction and Building Materials* 17(6-7): 439-446.

Razaqpur, A.G., Isgor, B.O., Greenaway, S. & Selley, A. 2004. Concrete contribution to the shear resistance of fiber reinforced polymer reinforced concrete members. *Journal of Composites for Construction* 8(5): 452-460.

Sherwood, E.G., Lubell, A.S., Bentz, E.C. & Collins, M.P. 2006. One-way shear strength of thick slabs and wide beams. *ACI Structural Journal* 103(6): 794-802.

Shioya, T., Iguro, M., Nojiri, Y., Akiyama, H. & Okada, T. 1989. Shear strength of large reinforced concrete beams. *Fracture Mechanics: Application to Concrete – ACI SP 118-12*: 259-279.

Taylor, H.P.J. 1972. Shear strength of large beams. *Journal of the Structural Division* 98(ST11): 2473-2490.

Tureyen, E.J. & Frosch, R.J. 2002. Shear tests of FRP-reinforced concrete beams without stirrups. *ACI Structural Journal* 99(4): 427-433.

Tureyen, E.J. & Frosch, R.J. 2003. Concrete shear strength: another perspective. *ACI Structural Journal* 100(5): 609-615.

Yoshida, Y. 2000. Shear reinforcement for large lightly reinforced concrete members. *MASc Thesis*. Toronto, Canada: Department of Civil Engineering, University of Toronto.

Yost, J.R., Gross, S.P. & Dinehart, D.W. 2001. Shear strength of normal strength concrete beams reinforced with deformed GFRP bars. *Journal of Composites for Construction* 5(4): 268-275.

Zhao, W., Maruyama, K. & Suzuki, H. 1995. Shear behavior of concrete beams reinforced by FRP rods as longitudinal and shear reinforcement. In L. Taerwe (ed.), *Non-Metallic (FRP) Reinforcement for Concrete Structures – FRPRCS-2; Proc. intern. symp., Ghent, Belgium, 23-25 August 1995*: 352-359. London: E&FN Spon.